Nonadaptive Rotor Speed Estimation of Induction Machine in an Adaptive Full-Order Observer

Marcin Morawiec ⬤, Paweł Kroplewski ⬤, and Ikechukwu Charles Odeh ⬤

Abstract—In the sensorless control system of an induction machine, the rotor speed value is not measured but reconstructed by an observer structure. The rotor speed value can be reconstructed by the classical adaptive law with the integrator. The second approach, which is the main contribution of this article, is the nonadaptive structure without an integrator. The proposed method of the rotor speed reconstruction is based on an algebraic relationship – the rank of the mathematical model of the observer system is not increased. However, the problem with the stabilization of the observer structure does exist. For near to zero rotor speed or in the regenerating mode of an induction machine, the speed observer structure can be unstable. Therefore, in this article, the new stabilization functions are proposed. The stability is provided by the Lyapunov theorem and the practical stability theorems in which the uncertainty of parameters is considered. In the proposed solution, the newly introduced stabilization functions guarantee observer stability during both the motoring and regenerating conditions at the chosen low rotor speed ranges and for different load torque values. All the theoretical considerations were confirmed by simulation and experimental tests during the chosen working modes and uncertainties of nominal parameters of the induction machine.

Index Terms—Adaptive estimation, induction machines, observers.

NOMENCLATURE

"^"	Estimated values.
"~"	Error of estimated values.
R_r, R_s	Rotor and stator resistance.
L_m	Main inductance.
$L_{s,r}$	Stator and rotor inductances.
J, T_L, T_e	Inertia, load, and electromagnetic torque.
$i_{s\alpha, \beta}$	Stator current vector components.
$u_{s\alpha, \beta}$	Stator voltage vector components.
$\psi_{r\alpha, \beta}$	Components of the rotor flux vector.
ω_r	Rotor angular speed.

I. INTRODUCTION

THE squirrel-cage induction machines (IM) are widely used in industrial drive systems due to their relatively simple construction and good dynamic properties. However, in order to achieve good performance and high dynamic a feedback closed-loop control system and an observer structure should be applied. Such a control system is named sensorless and it increases reliability in addition to the speed sensor. An estimator is used to reproduce the value of the state variables and rotor angular speed or position. Methods of rotor angular speed reproduction can be divided into three main groups [1]: Physical, algorithmic, and neural network. The large popular group is algorithmic in which the speed observer structure is based on the mathematical model of IM. Algorithmic methods include the state observer (full and reduced-order), e.g., [2], the full-order adaptive observer (AFO) [3]–[10], Kalman filter [11], [12], structures based on sliding technique [13]–[15], or backstepping structures [16]. Due to the simplicity of implementation, the large subgroups are structures based on the reference model reference adaptive system (MRAS) model [9], [10]. Similar to AFO, the rotor angular speed is obtained employing the classic adaptation law, using a PI integrator or proportional integration regulator. The other approach to the estimation of the state variables of IM is to extend the mathematical model of the machine with an additional state variable based on it (auxiliary state). The rotor speed can be obtained by using a suitable algebraic transformation of estimated state variables. The speed estimation method proposed in [11] and [12] is characterized by many observer tuning gains and a complicated form of stabilizing functions. In [13], the structure of the observer is based on the backstepping technique, which significantly reduced the number of tuning gains compared to [12], however, the observer model was extended by an additional integrator. Presented in [3] and [4], sensorless control system structures have often poor or limited performance in the low-speed regenerating region [6]–[8]. This region can be defined as follows: Zero rotor speed, operation near to zero speed (less than 10 r/min) with the nominal load torque value from motoring to

regenerating IM modes. The nonadaptive approach presented in [14]–[16], and [18] is more complicated and therefore can be unattractive in industrial applications. The AFO or MRAS speed observer structures are not complex like nonadaptive through which the computing time is shorter. However, the performance in the low-speed regenerating region cannot be always reached. Therefore in recent years, the stability problem of the AFO speed observer structures is studied. In [5], the feedback matrix was developed by the Routh–Hurwitz criterion to reduce the unstable region under low-speed regenerating mode. Stability analysis of AFO with the gains is presented in [5]–[8] using the Lyapunov theory. These gains were calculated to be adaptively dependent on the IM variables and parameters. Apart from the feedback matrix, the speed adaptive law has a significant role in the stability of IM. It was modified with an additional shift angle to improve stability [2]. Thus, the unstable regenerating region was significantly reduced. In [9], and [21], an auxiliary adaptive variable was introduced to stabilize the AFO. In summary, stabilization solutions for AFO structures presented in [1], [2], [5]–[7], and [9] can be divided into a few groups: 1) Through the suitable feedback matrix [5], [8], 2) introducing a shift angle to the classical speed estimation law [1], [2], 3) introducing the auxiliary variables [9], [21], and adaptation of the value of these variables. The comparative study of chosen methods was presented in [9]. Each of the approaches presented above has some advantages and disadvantages. In this article, the new approach for stabilization of AFO structure is presented. The idea is based on a modification of classical adaptation law and extending it by a simple introduced stabilization function. In a general form, the classical adaptive law contains a vector product of two different vectors [1], [2], [5], [7], [9], [10]. It follows the design procedure. However, the analysis proposed in Section III allows the use of the scalar product, and thus modification of classical adaptive law. The proposed solution gives an improvement of the IM properties in open as well as in the closed-loop control system.

In the AFO with classical adaptation law [1], [2], [5], [7], [9], [10] the rank of the speed observer is increased due to integrator structure. As is noticed in Section IV it is possible to obtain the value of the estimated rotor speed by using simply an algebraic equation. Through this, the rank of the observer does not change and the speed estimation process does not depend on the tuning gains of PI controller/integrator [5]. The nonadaptive speed estimation scheme presented in this article causes that the observer structure contains only four differential equations for the stator current vector and rotor flux vector components and the new formula from the value of rotor speed is reconstructed. The proposed solution is also the main contribution of this article and can be named: Nonadaptive full order observer (NAFO). The NAFO method of estimation presented in this article is the new solution and has never been presented before. The first main aim and contribution of this article are to show the algebraic approach to obtain the estimated value of rotor speed and the second is to show the way to enhance the AFO properties by introducing additional feedback (Section III).

The theoretical analysis includes an asymptotic Lyapunov theorem-based approach. If the IM reached the unobservable area (during the low speed and regenerating mode) and the persistent exciting condition is not satisfied then the practical stability is established [15]. The practical stability analysis is presented in Section III. All the presented theoretical issues are confirmed by simulation and experimental research on a 5.5-kW machine.

II. MATHEMATICAL MODEL OF INDUCTION MACHINE

The squirrel cage induction machine can be represented by the differential equations for the stator current vector and the rotor flux in $(\alpha\beta)$ related to the stator [14], [16], [18], [20]

$$\frac{di_{s\alpha}}{d\tau} = a_1 i_{s\alpha} + a_2 \psi_{r\alpha} + a_3 \omega_r \psi_{r\beta} + a_4 u_{s\alpha}$$

$$\frac{di_{s\beta}}{d\tau} = a_1 i_{s\beta} + a_2 \psi_{r\beta} - a_3 \omega_r \psi_{r\alpha} + a_4 u_{s\beta} \qquad (1)$$

$$\frac{d\psi_{r\alpha}}{d\tau} = a_5 \psi_{r\alpha} - \omega_r \psi_{r\beta} + a_6 i_{s\alpha}$$

$$\frac{d\psi_{r\beta}}{d\tau} = a_5 \psi_{r\beta} + \omega_r \psi_{r\alpha} + a_6 i_{s\beta} \qquad (2)$$

and the motion equation

$$\frac{d\omega_r}{d\tau} = \frac{L_m}{JL_r}(\psi_{r\alpha} i_{s\beta} - \psi_{r\beta} i_{s\alpha}) - \frac{1}{J}T_L \qquad (3)$$

where the following designations of coefficients have been introduced

$$a_1 = -\frac{R_s L_r^2 + R_r L_m^2}{L_r w_\sigma}, \ a_2 = \frac{R_r L_m}{L_r w_\sigma}, \ a_3 = \frac{L_m}{w_\sigma}, \ a_4 = \frac{L_r}{w_\sigma} \qquad (4)$$

$$a_5 = -\frac{R_r}{L_r}, \ a_6 = \frac{R_r L_m}{L_r}, \ w_\sigma = L_r L_s - L_m^2. \qquad (5)$$

It is assumed that the machine parameters are known and unchanging in time. In the next section, the mathematical model of IM (1)–(2) will be used for the construction of the AFO speed observer structure.

III. AFO SPEED OBSERVER OF INDUCTION MACHINE

The design procedure of AFO has been proposed for the first time in [3], [4]. Based on the mathematical model of IM for $(\alpha\beta)$ the AFO speed observer can be determined in the following form:

$$\frac{d\hat{i}_{s\alpha}}{d\tau} = a_1 \hat{i}_{s\alpha} + a_2 \hat{\psi}_{r\alpha} + a_3 \hat{\omega}_r \hat{\psi}_{r\beta} + a_4 u_{s\alpha} + \Delta_{i1} + v_\alpha \qquad (6)$$

$$\frac{d\hat{i}_{s\beta}}{d\tau} = a_1 \hat{i}_{s\beta} + a_2 \hat{\psi}_{r\beta} - a_3 \hat{\omega}_r \hat{\psi}_{r\alpha} + a_4 u_{s\beta} + \Delta_{i2} + v_\beta \qquad (7)$$

$$\frac{d\hat{\psi}_{r\alpha}}{d\tau} = a_5 \hat{\psi}_{r\alpha} - \hat{\omega}_r \hat{\psi}_{r\beta} + a_6 \hat{i}_{s\alpha} + v_{\psi\alpha} \qquad (8)$$

$$\frac{d\hat{\psi}_{r\beta}}{d\tau} = a_5 \hat{\psi}_{r\beta} + \hat{\omega}_r \hat{\psi}_{r\alpha} + a_6 \hat{i}_{s\beta} + v_{\psi\beta} \qquad (9)$$

where "^" an estimated values are marked, $v_{\alpha,\beta}$ and $v_{\psi\alpha,\beta}$ are stabilizing functions introduced to the structure and parametric

uncertain terms satisfying $|\Delta_{i1}| \leq \eta_1$ and $|\Delta_{i2}| \leq \eta_2$ (introduced only to the stator current derivatives).

The observer structure (6)–(9) is unstable if stabilizing functions are equal to zero [1]–[10] $v_{\alpha,\beta} = 0$, $v_{\psi\alpha,\beta} = 0$ (some observer poles are positive value). Therefore in the first stage to design the stabilizing functions by using the Lyapunov theorem, it is necessary to ensure the asymptotical stability of the proposed observer structure. The following Lyapunov function should be considered

$$V_1 = \frac{1}{2}\left(\tilde{i}_{s\alpha}^2 + \tilde{i}_{s\beta}^2 + \tilde{\psi}_{r\alpha}^2 + \tilde{\psi}_{r\beta}^2\right) > 0. \tag{10}$$

According to the procedure of determining the adaptive adjusting of rotor speed, the Lyapunov function (10) should be extended to the following form:

$$V = V_1 + \frac{1}{2\gamma}\tilde{\omega}_r^2 > 0 \tag{11}$$

and its derivative is negative determined

$$\dot{V}_1 = \tilde{i}_{s\alpha}\dot{\tilde{i}}_{s\alpha} + \tilde{i}_{s\beta}\dot{\tilde{i}}_{s\beta} + \tilde{\psi}_{r\alpha}\dot{\tilde{\psi}}_{r\alpha} + \tilde{\psi}_{r\beta}\dot{\tilde{\psi}}_{r\beta} + \frac{1}{\gamma}\dot{\tilde{\omega}}_r\tilde{\omega}_r \leq 0 \tag{12}$$

where

$$\tilde{\omega}_r = \hat{\omega}_r - \omega_r, \ \tilde{\psi}_{r\alpha,\beta} = \hat{\psi}_{r\alpha,\beta} - \psi_{r\alpha,\beta}, \ \tilde{i}_{s\alpha,\beta} = \hat{i}_{s\alpha,\beta} - i_{s\alpha,\beta} \tag{13}$$

and $\gamma > 0$ is the tuning gain.

Model of estimation errors for (6)–(9) by using (13) has the following form:

$$\frac{d\tilde{i}_{s\alpha}}{d\tau} = (a_1 + \Delta_{i1})\tilde{i}_{s\alpha} + a_2\tilde{\psi}_{r\alpha}$$
$$+ a_3(\tilde{\omega}_r\hat{\psi}_{r\beta} + \hat{\omega}_r\tilde{\psi}_{r\beta} - \tilde{\omega}_r\tilde{\psi}_{r\beta}) + v_\alpha \tag{14}$$

$$\frac{d\tilde{i}_{s\beta}}{d\tau} = (a_1 + \Delta_{i2})\tilde{i}_{s\beta} + a_2\tilde{\psi}_{r\beta}$$
$$- a_3(\tilde{\omega}_r\hat{\psi}_{r\alpha} + \hat{\omega}_r\tilde{\psi}_{r\alpha} - \tilde{\omega}_r\tilde{\psi}_{r\alpha}) + v_\beta \tag{15}$$

$$\frac{d\tilde{\psi}_{r\alpha}}{d\tau} = a_5\tilde{\psi}_{r\alpha} - (\tilde{\omega}_r\hat{\psi}_{r\beta} + \hat{\omega}_r\tilde{\psi}_{r\beta} - \tilde{\omega}_r\tilde{\psi}_{r\beta}) + a_6\tilde{i}_{s\alpha} + v_{\psi\alpha} \tag{16}$$

$$\frac{d\tilde{\psi}_{r\beta}}{d\tau} = a_5\tilde{\psi}_{r\beta} + (\tilde{\omega}_r\hat{\psi}_{r\alpha} + \hat{\omega}_r\tilde{\psi}_{r\alpha} - \tilde{\omega}_r\tilde{\psi}_{r\alpha}) + a_6\tilde{i}_{s\beta} + v_{\psi\beta}. \tag{17}$$

The observer structure will be asymptotically stable if the Lyapunov theorem is satisfied. After substitution, the derivative of the function (12) is as follows:

$$\dot{V} = a_5(\tilde{\psi}_{r\alpha}^2 + \tilde{\psi}_{r\beta}^2) + \tilde{\omega}_r\left(\begin{array}{c}\frac{1}{\gamma}\dot{\hat{\omega}}_r - a_3\hat{\psi}_{r\alpha}\tilde{i}_{s\beta} + \\ + a_3\hat{\psi}_{r\beta}\tilde{i}_{s\alpha}\end{array}\right) \leq 0 \tag{18}$$

wherein (6)–(9) the observer stabilizing functions are introduced and should be taken

$$v_\alpha = -(c_\alpha + \Delta_{i1})\tilde{i}_{s\alpha},$$
$$v_\beta = -(c_\alpha + \Delta_{i2})\tilde{i}_{s\beta} \tag{19}$$
$$v_{\psi\alpha} = -c_{\psi1}\tilde{i}_{s\alpha} + c_\psi\hat{\omega}_r\tilde{i}_{s\beta},$$

$$v_{\psi\beta} = -c_{\psi1}\tilde{i}_{s\beta} - c_\psi\hat{\omega}_r\tilde{i}_{s\alpha} \tag{20}$$

where it is assumed that $\hat{\psi}_{r\alpha,\beta} \approx 0$, and the observer gains c_α is the function of the a_1 parameter ($c_\alpha = f(a_1) > 0$) as well as $c_\psi = f(a_3) > 0$, whereas $c_{\psi1} \geq 0$, $a_5 < 0$.

The uncertain terms are bounded $|\Delta_{i1}| \leq \eta_1, |\Delta_{i2}| \leq \eta_2$ and under the above assumptions, the value of stabilizing functions defined in (19)–(20) are not accurately determined due to $c_\alpha = f(a_1) > 0$, $c_\psi = f(a_3) > 0$. It means that c_α and c_ψ are the function of the IM parameters (a_1 and a_3, respectively). Therefore, the observer system is considered as the structure with uncertain and bounded parameters.

The value of rotor speed can be reproduced from an adaptive mechanism by using the integrator [1], [10]

$$\frac{d\hat{\omega}_r}{d\tau} = -\gamma a_3(\tilde{i}_{s\alpha}\hat{\psi}_{r\beta} - \tilde{i}_{s\beta}\hat{\psi}_{r\alpha}) \tag{21}$$

assuming that $\dot{\omega}_r = 0$ (the real speed is considered here to be constant), therefore

$$\dot{\tilde{\omega}}_r = \dot{\hat{\omega}}_r \tag{22}$$

Estimation of rotor speed from the law of adaptation (21) can lead to deterioration of properties of the observer structure due to the open loop of the integrator, as noted in [19] for the first-order system. It influences on decreasing the sensorless control system properties, which loses the stability near to the zero speed or for generating IM mode. It will be seen in the next section during the stability analysis. Therefore, it was proposed to add feedback to improve system stability. The adaptive mechanism has the form

$$\frac{d\hat{\omega}_r}{d\tau} = -\gamma a_3(\tilde{i}_{s\alpha}\hat{\psi}_{r\beta} - \tilde{i}_{s\beta}\hat{\psi}_{r\alpha} + \gamma_1\hat{\omega}_r) \tag{23}$$

where $(\gamma, \gamma_1) > 0$.

The coupling $(-\gamma_1\hat{\omega}_r)$ leads to improved system stability, however, it does not immunize the observer system, which may be susceptible to, e.g., external disturbances that were not taken into account at the design stage (variation of machine parameters during operation and others). Therefore, the author of this article would like to propose three different approaches for the improvement of rotor speed estimation.

Proposal 1: Taking into account any two vectors defined in them (1)–(2) or (6)–(9) which are state estimates in the system or estimation errors, between which the following relationships occur:

$$\vec{a} \times \vec{b} \neq 0 \tag{24}$$

$$\vec{a} \cdot \vec{b} \cong 0 \tag{25}$$

where $\vec{a} \times \vec{b}$ means the vector product (cross product) of two vectors, $\vec{a} \cdot \vec{b}$ means the scalar product, the law of adaptation from which the rotor angular speed can be reconstructed is generalized to the form

$$\frac{d\hat{\omega}_r}{d\tau} = \gamma(\vec{a} \times \vec{b} - \gamma_1\hat{\omega}_r) \tag{26}$$

where $(\vec{a}, \vec{b})$ is the selected pair of two vectors in the system.

The sign of expression (26) as well as additional parameters that may appear (26) depending on the designed structure and

directly result from the Lyapunov function from which the stability of the observer is examined.

Proposal 2: A robust law of adaptation can be obtained by introducing feedback, which makes expression (26) have the following form:

$$\frac{d\hat{\omega}_r}{d\tau} = \gamma \left(\vec{a} \times \vec{b} - \gamma_1 \hat{\omega}_r (\vec{a} \cdot \vec{b}) \right). \tag{27}$$

Considering the ideal case, in which the vectors are perpendicular to each other, form (26) (for $\gamma = 0$ that is classical control law) is obtained, while in the case when $\vec{a} \cdot \vec{b} \neq 0$ additional feedback arises compensating for uncertainties interference and improving the robustness of the observer system. The adaptation mechanism (23) in the considered case including (27) has the form

$$\frac{d\hat{\omega}_r}{d\tau} = -\gamma a_3 \left(\tilde{i}_{s\alpha} \hat{\psi}_{r\beta} - \tilde{i}_{s\beta} \hat{\psi}_{r\alpha} + k_c s_\omega \right) \tag{28}$$

where

$$s_\omega = \tilde{i}_{s\alpha} \hat{\psi}_{r\alpha} + \tilde{i}_{s\beta} \hat{\psi}_{r\beta} \tag{29}$$

and

$$k_c = k_f \hat{\omega}_r, \, k_f > 0. \tag{30}$$

It is worth noting that for the very low-speed range the feedback $k_c = k_f \hat{\omega}_r \approx 0$ introduced in (28), therefore it is better to use signum function of $\hat{\omega}_r$ or k_f calculated from the reference rotor speed what is presented in Remark 1. It yields that the feedback $(k_c s_\omega)$ in (28) will be in the following form $(k_c k_f s_\omega)$ in which the k_f is only the sign of the rotor speed (like in Remark 1).

In the next step, it will be shown that for the system (1)–(2), the AFO observer (6)–(9) with the proposed stabilization functions (19)–(20), can exponentially converge vectors values $\hat{\vec{i}}_s$ to $\vec{i}_s$ and $\hat{\vec{\psi}}_r$ to $\vec{\psi}_r$. Taking into account the theorems on the practical stability presented in [14] and [15], the stability analysis can be proved. Substituting (19)–(20), and (28) to the derivative of (11), one obtains

$$\dot{V} = a_5(\tilde{\psi}_{r\alpha}^2 + \tilde{\psi}_{r\beta}^2) + \delta_\alpha \left| \tilde{i}_{s\alpha} \right| + \delta_\beta \left| \tilde{i}_{s\beta} \right| + (\delta_{\psi\alpha} + \delta_{\psi 1\alpha}) \left| \tilde{\psi}_{r\alpha} \right|$$
$$+ (\delta_{\psi\beta} + \delta_{\psi 1\beta}) \left| \tilde{\psi}_{r\beta} \right| + \delta_c \left| \tilde{\omega}_r \right| + \Delta_{i1} \left| \tilde{i}_{s\alpha} \right| + \Delta_{i2} \left| \tilde{i}_{s\beta} \right| \leq -\mu V + \kappa \tag{31}$$

with $\delta_{\alpha 1}, \delta_{\alpha 2}, \delta_{\psi\alpha}, \delta_{\psi\beta}, \delta_{\psi 1\alpha}, \delta_{\psi 1\beta}, \delta_c > 0$ and $\tilde{i}_{s\alpha} \leq \varepsilon_1$, $\tilde{\psi}_{r\alpha,\beta} \leq \varepsilon_2$, $\tilde{\omega}_r \leq \varepsilon_3$, $\varepsilon_{1,2,3} \ll 1$ are sufficient small real numbers $\varepsilon_{1,2,3} > 0$ and where

$$c_{\alpha 1} = \max\{a_1 \tilde{i}_{s\alpha} + a_2 \tilde{\psi}_{r\alpha} - \Delta_{i1}\} + \delta_{\alpha 1} \tag{32}$$

$$c_{\alpha 2} = \max\{a_1 \tilde{i}_{s\beta} + a_2 \tilde{\psi}_{r\beta} - \Delta_{i2}\} + \delta_{\alpha 2} \tag{33}$$

$$c_{\psi\alpha} = \max\{a_3 \hat{\omega}_r \tilde{i}_{s\beta}\} + \delta_{\psi\alpha} \tag{34}$$

$$c_{\psi\beta} = \max\{a_3 \hat{\omega}_r \tilde{i}_{s\beta}\} + \delta_{\psi\beta} \tag{35}$$

$$c_{\psi 1\alpha} = \max\{a_6 \tilde{i}_{s\alpha}\} + \delta_{\psi 1\alpha} \tag{36}$$

$$c_{\psi 1\beta} = \max\{a_6 \tilde{i}_{s\beta}\} + \delta_{\psi 1\beta} \tag{37}$$

$$k_c = \max\{\gamma a_3 (\tilde{i}_{s\alpha} \hat{\psi}_{r\beta} - \tilde{i}_{s\beta} \hat{\psi}_{r\alpha}) \big/ s_\omega\} + \delta_c \tag{38}$$

and for $s_\omega \neq 0$.

The AFO will be practical stable if the Lyapunov function derivatives are

$$\dot{V} \leq -\mu V + \kappa \tag{39}$$

where

$$\mu = \min \left(\delta_{\alpha 1} - \frac{1}{2\xi_1^2}, \delta_{\beta 1} - \frac{1}{2\xi_2^2}, \sqrt{2}(\delta_{\psi\alpha} + \delta_{\psi 1\alpha}), \right.$$
$$\left. \sqrt{2}(\delta_{\psi\beta} + \delta_{\psi 1\beta}), \sqrt{2}\delta_c \right) \tag{40}$$

and $\kappa = 0.5(\xi_1^2 \eta_1^2 + \xi_2^2 \eta_2^2), \forall \xi_i \in (0,1), i = 1,2$.

For an ideal condition (all the IM parameters are known and constant and $\kappa = 0$) it can be assumed that $c_\alpha = c_{\alpha 1} = c_{\alpha 2}$, $c_{\psi 1} = c_{\psi 1\alpha} = c_{\psi 1\beta}$, $c_\psi = c_{\psi\alpha} = c_{\psi\beta}$, and the above condition implies the convergence of vectors values $\hat{\vec{i}}_s$ to $\vec{i}_s$ and $\hat{\vec{\psi}}_r$ to $\vec{\psi}_r$ in finite time, noted as t_1. Consequently, for $\hat{\psi}_{r\alpha}^2 + \hat{\psi}_{r\beta}^2 > 0$, the estimated rotor angular speed $\hat{\omega}_r$ converges exponentially to ω_r in finite time $t > t_2 > t_1$. For $\kappa \neq 0$ it can be proved as in [15] that the estimates of the observer converge to the set of radius κ/μ depends on the IM parameters.

It should be noted that for zero synchronous frequency $\omega_o = 0$, the IM is supplied by dc voltage, therefore the persistent exciting condition is not satisfied [5], [23] and the observer structure is unstable.

IV. NONADAPTIVE FULL ORDER OBSERVER

The adaptation mechanism according to [1]–[11] and (28) requires the use of the integrator structure (to extend the observer structure to an auxiliary state [9], [21] and based on this, estimation of rotor speed). Therefore, the rank of the speed observer structure is increased due to the integrator structure. Another approach to determine the value of the rotor speed can be the nonadaptive mechanism. Considering (21) it can be presented as a combination of two expressions

$$\frac{d\tilde{\omega}_r}{d\tau} = -\gamma a_3 \left(\underbrace{\tilde{i}_{s\alpha} \hat{\psi}_{r\beta}}_{I} - \underbrace{\tilde{i}_{s\beta} \hat{\psi}_{r\alpha}}_{II} \right). \tag{41}$$

If the individual expressions are considered separately, then it can define the following equations that should occur in these expressions so that the observer structure is kept up with the object. Under the assumption that in the steady state the following equality holds:

$$I : \tilde{i}_{s\alpha} \equiv \gamma^{-1} \hat{\omega}_r \hat{\psi}_{r\beta} \tag{42}$$

$$II : \tilde{i}_{s\beta} \equiv -\gamma^{-1} \hat{\omega}_r \hat{\psi}_{r\alpha} \tag{43}$$

then in the adjusting (estimation) process, values of estimated stator current error α-component can be equivalent to $\gamma^{-1}(\hat{\omega}_r \hat{\psi}_{r\beta})$ and the second β-component to $\gamma^{-1}(-\hat{\omega}_r \hat{\psi}_{r\alpha})$.

In the next step, both sides of (34) and (35) should be multiplied by $\hat{\psi}_{r\beta}$ and $\hat{\psi}_{r\alpha}$, respectively, added to each other and

transformed, in such a way as to obtain the following formula:

$$\hat{\omega}_r = \gamma \frac{\tilde{i}_{s\alpha}\hat{\psi}_{r\beta} - \tilde{i}_{s\beta}\hat{\psi}_{r\alpha}}{\hat{\psi}_r^2}. \tag{44}$$

After substitution of (44) to (41) and after assuming (22), the solution of (41) is

$$\tilde{\omega}_r = \tilde{\omega}_{r0} e^{-\vartheta\tau} \tag{45}$$

where $\hat{\psi}_r^2 = \hat{\psi}_{r\alpha}^2 + \hat{\psi}_{r\beta}^2 \neq 0$, $\tilde{\omega}_{r0} \neq 0$, and under the assumption (22).

In (45) it has been shown that for $\tau \to \infty$, the rotor speed estimation error will exponentially decay to zero, with the rate of convergence equal to $\vartheta = a_3\hat{\psi}_r^2$ (assuming an ideal state in which all the IM parameters are known and constant as well as $(\Delta_{i1}, \Delta_{i2}) = 0$).

Proposal 3: To improve the properties of rotor angular speed estimation (44), a feedback coupling should be introduced in a similar way as in (27), which is a scalar product of vectors. If (42) and (43) are multiplied by components $\hat{\psi}_{r\beta}$ and $\hat{\psi}_{r\alpha}$, respectively, and (42)–(43) by $\hat{\psi}_{r\alpha}$ and $\hat{\psi}_{r\beta}$ then the following is obtained:

$$\tilde{i}_{s\alpha}\hat{\psi}_{r\beta} - \tilde{i}_{s\beta}\hat{\psi}_{r\alpha} \equiv \gamma^{-1}\hat{\omega}_r\hat{\psi}_r^2 \tag{46}$$

$$\tilde{i}_{s\alpha}\hat{\psi}_{r\alpha} + \tilde{i}_{s\beta}\hat{\psi}_{r\beta} \equiv 0. \tag{47}$$

By adding the terms (46) to (47) on both sides and after transformation, one obtains

$$\hat{\omega}_r = \gamma \frac{\tilde{i}_{s\alpha}\hat{\psi}_{r\beta} - \tilde{i}_{s\beta}\hat{\psi}_{r\alpha} + k_c k_f s_\omega}{\hat{\psi}_r^2} \tag{48}$$

where $\gamma = 1$ p.u. and s_ω is defined in (29).

The value of the rotor speed can be determined from (48) from the developed algebraic expression.

The main advantage of using the nonadaptive approach is that the rank of the observer model is the same as the rank of IM model (both are equal to 4, of course under the assumption of the electromagnetic part of equations) and above all, the exclusion of γ coefficient from the tuning process (because $\gamma = 1$ p.u.), which has an important meaning in AFO structure and it influences the stability of AFO speed observer structure.

Remark 1: The function k_c occurring in (28) and (48) in some operating ranges of the machine (e.g., during zero speed and load torque changes) can be replaced by a discontinuous form depending on the reference speed value or vector product specified for the stator voltage and rotor flux vectors

$$k_f = \text{sgn}(.) = \begin{cases} 1 (u_{s\beta}\hat{i}_{s\alpha} - u_{s\alpha}\hat{i}_{s\beta}) < 0 \\ -1 (u_{s\beta}\hat{i}_{s\alpha} - u_{s\alpha}\hat{i}_{s\beta}) \geq 0 \end{cases} \tag{49}$$

in the other cases, it can be satisfied for

$$k_f = \text{sgn}(.) = \begin{cases} 1 (\tilde{i}_{s\alpha}\hat{\psi}_{r\beta} - \tilde{i}_{s\beta}\hat{\psi}_{r\alpha}) < 0 \\ -1 (\tilde{i}_{s\alpha}\hat{\psi}_{r\beta} - \tilde{i}_{s\beta}\hat{\psi}_{r\alpha}) \geq 0 \end{cases} \tag{50}$$

where the expression in the pole of sgn(.) is the numerator of (44).

Remark 2: The vectors of the system (1)–(2) and the AFO observer (6)–(9) can be represented in $(\alpha\beta)$ stationary coordinate system what can be seen in Fig. 1. It can be noticed that the
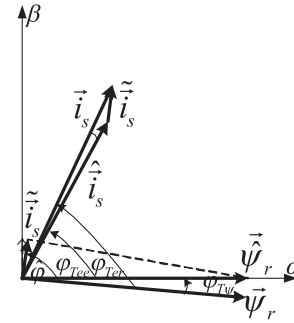

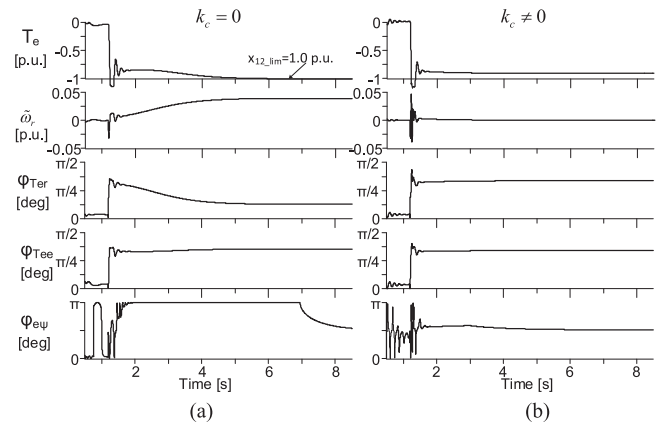Fig. 1. Vectors in $(\alpha\beta)$ stationary system and their angles.

Fig. 2. Regenerating mode of IM, reference speed is 0.05 p.u., after 1-s load torque is injected to 0.8 p.u for $k_c = 0$ (Fig. 2(a)), $k_c \neq 0$ [Fig. 2(b)].

vector product of the two vectors $\vec{\tilde{i}}_s$ and $\hat{\vec{\psi}}_r$ is equal to $(\tilde{i}_{s\alpha}\hat{\psi}_{r\beta} - \tilde{i}_{s\beta}\hat{\psi}_{r\alpha})$ and the angle between these vectors are in stationary almost $\pi/2$. Therefore its value is not equal to zero but it can be defined like in (46), hence the vector product is equal to $\gamma^{-1}\hat{\omega}_r\hat{\psi}_r^2$. Whereas the scalar product defines the angle between vectors $\vec{\tilde{i}}_s$ and $\hat{\vec{\psi}}_r$, hence it is $(\cos\hat{\varphi})$ therefore this value is about zero as was noted in (47) but it allows to stabilize the observer system and to minimize the shift angle between the real values of vectors and estimated (of course it is assumed that the shift angle between $\hat{\vec{i}}_s$ and $\hat{\vec{\psi}}_r$ remains not changed).

Remark 2 can be supported by the simulation results of the AFO structure in which the $k_c = 0$ [Fig. 2(a)] and $k_c \neq 0$ [Fig. 2(b)]. If the factor k_c is set to zero then the error of estimated rotor speed increases above 0.05 p.u. until the electromagnetic torque value reaches the upper bound of limit (in the simulation it is limited to $x_{12\cdot\text{lim}} = 1.0$).

In Fig. 2 the following values of the shift angle are presented: $\varphi_{Ter} \triangleleft(\vec{i}_s, \vec{\psi}_r)$ - real (measured) values of vectors, $\varphi_{Tee} \triangleleft(\hat{\vec{i}}_s, \hat{\vec{\psi}}_r)$ - estimated by the AFO structure, $\varphi_{e\psi} \triangleleft(\vec{\tilde{i}}_s, \vec{\psi}_r)$ - real and estimated values of rotor flux vectors

For $k_c = 0$, $\varphi_{Ter} \neq \varphi_{Tee}$, and $\varphi_{e\psi}$ are limited to π. For $k_c \neq 0$ $\varphi_{Tee}\sim = \varphi_{Ter}$ and $\varphi_{e\psi}\sim = \pi$, what is visible in Fig. 2(a), (b).

Remark 3: It worth noticing that the angle $\hat{\varphi} \triangleleft (\vec{i}_s, \vec{\psi}_r)$ between the vectors $\vec{i}_s$ and $\vec{\psi}_r$ is close to $\pi/2$, although the others have different values dependent on IM working points. The vector which is the normal vector (created on the base of vector product) is perpendicular to vectors $\vec{i}_s$ and $\vec{\psi}_r$ in an ideal case but in the practical application, it can have a different value $\pi/2$. During the IM working the vectors deviated from each other and to minimize the proper values of angle shifts between estimated vectors by AFO and the real values (which are nonmeasured), the estimated rotor speed should contain the additional stabilizing term, which was determined in (29). The estimated rotor speed from (28) or (48) tunes the observer system, influences vectors values and their mutual position. Therefore, to obtain improvement observer properties, the k_c factor should be $k_c \neq 0$ for the whole IM working condition.

Remark 4: The values in (29) introduced to the estimation law (28) and (48) should be filtrated using the low-pass filter to prevent the algebraic loop and smooth values of estimated rotor speed. The filter time constant is $1/T_i = 1/\vartheta$ p.u. due to the form of (45) (ϑ coefficient influences the rate of speed error decay to zero) and in the simulation was set to $1/T_i = 1/(a_3 \hat{\psi}_r^2) \approx 0.2$ (for $a_3 = 5.08$ p.u. and $\hat{\psi}_r^2 = 1$ p.u.). However, to minimize the oscillation in the observer structure, it is assumed that $1/T_i \approx 0.01 a_3$ (in the laboratory stand the coefficient 0.01 was arbitrarily introduced and its value allows to minimize of oscillations of estimated variables by the observer structure which can be a consequence of variability of IM during the working (from motoring mode to regenerating) as well as additional phenomena which are omitted).

V. STABILITY ANALYSIS OF THE OBSERVER STRUCTURE

The stability property of the speed estimation in AFO structure was studied in [5] for the different operations of IM. Authors in [5] applied the Routh–Hurwitz criterion to obtain sufficient conditions for stable speed estimation. In [5] the design strategy for adaptation gain γ is shown. Based on studies presented in [5] the stability analysis of the ideal speed observer of the IM model is carried out. In this analysis (feedback gains) observer tuning gains which are in (19)–(20) are chosen by pole placement method of linearized observer structure. These gains influence the speed of observer convergences. The tuning gains can be specified from the model of the observer errors (14)–(17) (nonlinear approach) or the observer structure (6)–(9) can be linearized near equilibrium points. In the drive system, the second approach is more desirable than the first, due to the possibility of taking into account specific machine working points in which it can be unstable. To examine the impact of the observer gains on the stability range, the nonlinear observer system (6)–(9) is linearized near the equilibrium point. The linearized system has the general form

$$\frac{d}{dt} \Delta \mathrm{x}(t) = \mathrm{A} \Delta \mathrm{x}(t) + \mathrm{B} \Delta \mathrm{u}(t) \qquad (51)$$
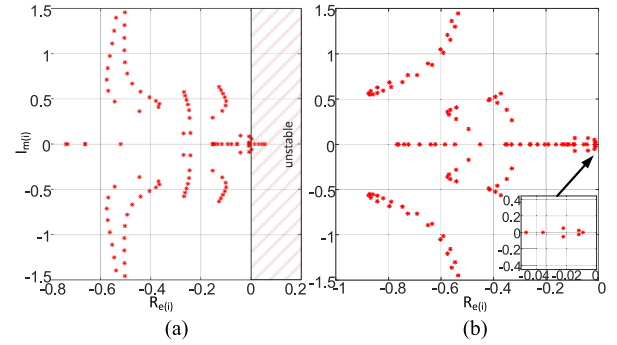
Fig. 3.   Spectrum of matrix **A** of the linearized observer system. The rotor speed is changing from -1.0 to 1.0 p.u., $T_L = 0.8$ p.u., a) $c_\alpha = 5$, $c_\psi = 0.5$, $\gamma = 0.5$, $\gamma_1 = 0$, $k_c = 0$. b) $c_\alpha = 5$, $c_\psi = 0.5$, $\gamma = 0.5$, $\gamma_1 = 1$, $k_c = 0.5$.

where **A**, **B** are the Jacobian matrices and $\Delta \mathrm{x}(t) = [\tilde{i}_{sd}, \tilde{i}_{sq}, \tilde{\psi}_{rd}, \tilde{\psi}_{rq}, \tilde{\omega}_r]^T$, $\Delta \mathrm{u}(t)$ is treated as known control inputs.

The estimator system is oriented with the rotor flux vector $\vec{\psi}_r$, so $|\vec{\psi}_r| = \sqrt{\psi_{rd}^{*2} + \psi_{rq}^{*2}}$ and the stator current vector components and ω_ψ can be treated as follows:

$$i_{sd} = \frac{\psi_{rd}^*}{L_m}, = \frac{T_L^*}{a_4 \psi_{rd}^*}, \omega_\psi^* = a_6 \left(\frac{i_{sq}}{\psi_{rd}^*} + \hat{\omega}_r^* \right). \qquad (52)$$

Taking into account the model of observer structure errors and its linearization near the equilibrium point, matrix **A** is defined as follows:

$$\mathrm{A} = \begin{bmatrix} a_1 + c_\alpha & \omega_\psi & a_2 & a_3 \hat{\omega}_r^* & a_3 \hat{\psi}_{rq}^* \\ -\omega_\psi & a_1 + c_\alpha & -a_3 \hat{\omega}_r^* & a_2 & -a_3 \hat{\psi}_{rd}^* \\ a_6 & -c_\psi \hat{\omega}_r^* & a_5 & \omega_s & -\hat{\psi}_{rq}^* \\ c_\psi \hat{\omega}_r^* & a_6 & -\omega_s & a_5 & \hat{\psi}_{rd}^* \\ \gamma a_7 & -\gamma a_8 & 0 & 0 & \gamma_1 \end{bmatrix} \qquad (53)$$
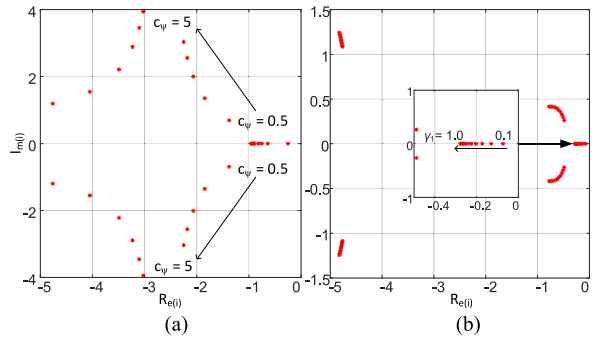
where $\omega_s = \omega_\psi^* - \hat{\omega}_r^*$, $a_7 = \hat{\psi}_{rq}^* + k_c \hat{\psi}_{rd}^*$, $a_8 = \hat{\psi}_{rd}^* - k_c \hat{\psi}_{rq}^*$, and $(*)$ means the values for equilibrium points.

To show the influence of tuning gain k_c the following working points are assumed: $\hat{\psi}_{rq}^* \approx 0.06$ p.u., $\hat{\psi}_{rd}^* = \sqrt{1 - \hat{\psi}_{rq}^{*2}}$. The stability analysis of the AFO speed observer was presented in detail in [1]–[11]. This article presents how the different tuning gains, in additional feedback, influence the stability range of linearized observer system without any disturbances. The tuning gains are chosen arbitrarily (extreme values of the tuning gains are chosen) to illustrate how the value of different gains influence the placement of observer poles. The analysis in which the bode plots of the AFO system for different IM working conditions (motoring, regenerating), zero freq. and for the corner freq. of adaptation PI controller gains, and taking into account feedback gains was presented by the authors in the paper [5].

As mentioned in Section III, to stabilize the AFO structure, the coefficients k_c and γ_1 were introduced. These coefficients are represented in (53) by a_7 and a_8. In Fig. 3(a), the spectrum of the matrix of the linearized observer system during the rotor speed changing (machine reverse) from -1.0 to 1.0 p.u are shown. The machine is loaded nominally $T_L = 0.8$ p.u. Fig. 3(a)
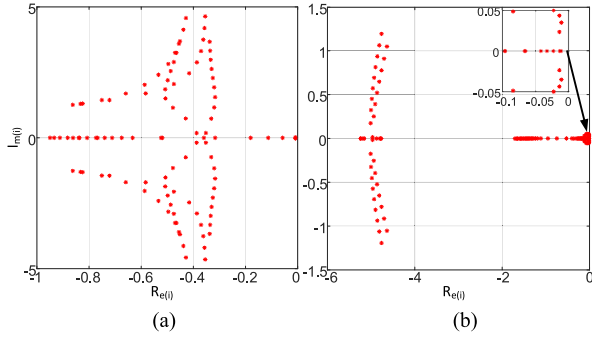
Fig. 4. Spectrum of matrix **A** of the linearized observer system. The rotor speed is changing from -1.0 to 1.0 p.u., $T_L = 0.8$ p.u., a) $c_\alpha = 0.5$, $c_\psi = 0.5$, $\gamma = 0.5$, $\gamma_1 = 1$, $k_c = 0.5$. b) $c_\alpha = 5$, $c_\psi = 0.5$, $\gamma = 0.1$, $\gamma_1 = 1$, $k_c = 0.5$.
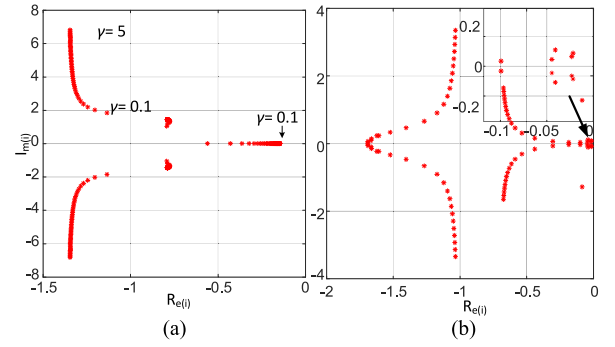

Fig. 6. Spectrum of matrix **A** of the linearized AFO observer system for $T_L = 0.8$ p.u., $c_\alpha = 1.0$, $c_\psi = 0.2$, $k_c = 6$. (a) During the changes $\gamma = 0.1 \ldots 5.0$, $\omega_r = 1$. b) During the changes $\omega_r = -1 \ldots 1$ in NAFO.

Fig. 5. Spectrum of matrix **A** of the linearized observer system for $\omega_r = 1$, $T_L = 0.8$ p.u., $c_\alpha = 0.5$, $\gamma = 0.5$, during the changes: a) $(c_\psi, k_c) = 0.5 \ldots 5.0$, b) $\gamma_1 = 0.1 \ldots 1$, $c_\psi = 0.2$, $k_c = 0.5$.

shows that the AFO structure is unstable if $(\gamma_1 = 0, k_c = 0)$ – during the regenerating mode a few of the observer poles have the positive value. This case was presented in [1]–[11] (for the feedback matrix gains equal to zero, however, for $\gamma_1 = 0$, $k_c = 0$). To stabilize the AFO structure, the feedback in the integrator structure is added. Therefore for $\gamma_1 = 1$ and $k_c = 0.5$ and changes of the rotor speed from -1 to 1 and $T_L = 0.8$ p.u., all the observer poles have negative values [Fig. 3(b)]. This test confirms that the AFO structure is stable and the unstable region is not reached.

In Fig. 4 the spectrum of the matrix of the linearized observer is presented for: a) $c_\alpha = 0.5$ and b) $c_\alpha = 5$ during the changing of rotor speed from -1.0 to 1.0 p.u. and $T_L = 0.8$ p.u. The observer structure is stable (the poles have negative values).

In Fig. 5 the spectrum of the matrix of the linearized observer system is presented during the changes of the following coefficients: a) $(c_\psi, k_c) = 0.5 \ldots 5.0$ and b) $\gamma_1 = 0.1 \ldots 1$ p.u., for the nominal value of rotor speed and load torque. The pole placement presented in Fig. 1–5 show that the observer system is stable for $\gamma_1 > 0$ and different changes of other gains: $c_\alpha = 0.5$ and 5.0 (Fig. 4) and $(c_\psi, k_c) = 0.5 \ldots 5.0$ [Fig. 5(a)]. If $\gamma_1 = 0$ then the gain k_c in (30) is equal to zero and it yields to open integrator structure. In Fig. 3, it has been confirmed that the additional term introduced in (28), defined in (29), allows for the displacement of poles from unstable region to the stable one. However, the

oscillations of the state estimations may occur if the different values of the tuning gains will be chosen. To minimize these oscillations, the imaginary values of poles should be closest to zero as shown in Figs. 3(b)–5. An explanation of the meaning of the function defined in (29), from the point of view of the physics of the phenomenon, is presented in Sections III and IV. Influences of changes of γ on observer stability from 0.1 to 5.0 for $\omega_r = 1.0$ and $T_L = 0.8$ p.u. were presented in Fig. 6. For $\gamma = 5.0$ (for increasing values of γ) the oscillation in the observer system occurs (imaginary values poles move away from zero). The deeper analysis of the design of γ tuning gains was presented in [5]. For the value of $\gamma > 1.0$, the observer structure is stiffer, however, the oscillations of the estimation values can occur.

In the case of NAFO speed estimation scheme (48), the stability analysis is presented below. In (48) there is k_c coefficient which influences the placement of the poles of the linearized observer structure. Therefore, the matrix $\Delta x(t)$ is considered as $\Delta \mathrm{x}(t) = [\tilde{i}_{sd}, \tilde{i}_{sq}, \tilde{\psi}_{rd}, \tilde{\psi}_{rq}]^T$ as well as the matrix **A** has determined according to $\Delta \mathrm{x}(t)$ (without last row and column).

To consider the $(k_c s_\omega)$ in the linearized structure the value of reference speed can be calculated as $\hat{\omega}_r^* = \hat{\omega}_r^* + k_c s_\omega^*$ and $s_\omega^* = \tilde{i}_{sd}^* \psi_{rd}^* + \tilde{i}_{sq}^* \psi_{rq}^* \approx 0.05$ p.u. The spectrum of the matrix is presented in Fig. 6(b). The poles of the linearized structure always have negative values, however, if $k_c = 0$ the poles are moving toward zero (please compare Fig. 2(a) for $k_c = 0$ to Fig. 2(b) for $k_c \neq 0$). Furthermore, the value of the tuning gain k_c can be determined from (38)

$$k_c = \max\left\{\left|a_3\left(\tilde{i}_{sd}^* \hat{\psi}_{rq}^* - \tilde{i}_{sq}^* \hat{\psi}_{rd}^*\right)\right/ s_\omega^*\right|\right\}. \tag{54}$$

For $\gamma = 1$, $a_3 = 5.08$ p.u., $\hat{\omega}_r^* = 1$, $T_L = 0.8$, $\max\{\tilde{i}_{sd}^*, \tilde{i}_{sq}^*\} = 0.05$ and the other values from (52), the minimum value of $k_c \approx 4.5$ p.u.

In Fig. 7 influence of changes value of k_c from 0 to 5.0 is shown. It is visible in Fig. 7(a), that for $k_c < 0.5$ the AFO structure is unstable (for the small speed value of rotor speed and regenerating mode), while for the same working points the NAFO structure is stable (even if $k_c = 0$, however, the observer properties are not satisfied). This property of NAFO structure is confirmed in the simulation results presented in Fig. 8.
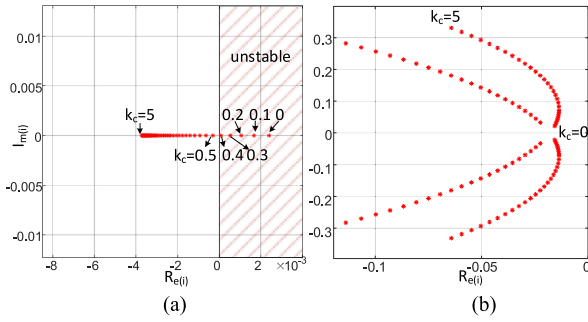
Fig. 7. Spectrum of matrix **A** of the linearized observer system for $\omega_r = 0.03$, $T_L = -0.8$, $c_\alpha = 1.0$, c_ψ, $= 0.2$, $k_c = 0 \ldots 5$ p.u.. (a) AFO. (b) NAFO.
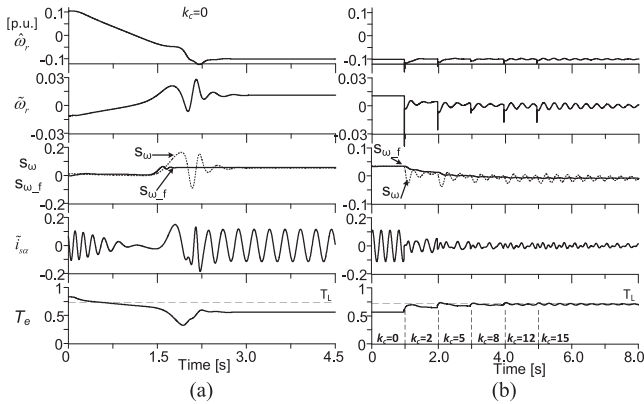

Fig. 8. IM is reversing from 0.1 to -0.1 p.u., the constant value of load torque is set $T_L = 0.7$ p.u.. a) $k_c = 0$. b) Various value of k_c from 0 to 15. Simulation results.

Fig. 9. Speed-torque trajectories for NAFO (green—-estimated rotor speed, red—-unstable area, black—-reference rotor speed value), $c\alpha = 1.0$, $c\psi = 0.2$, $kc = 8$.

TABLE I
INDUCTION MACHINE PARAMETERS AND REFERENCES UNIT

Symbol	Quantity	Values
R_{sN}	stator resistance	2.92 Ω/0.035 p.u.
R_{rN}	rotor resistance	3.36 Ω/0.032 p.u.
L_{mN}	magnetizing inductance	0.422 H/1.95 p.u.
L_s, L_r	stator and rotor inductance	0.439 H/2.04 p.u.
L_σ	leakage inductance	0.017 H/0.09 p.u.
P_n	nominal power	5.5 kW
I_n	nominal stator current (Y)	11 A
U_n	nominal stator voltage (Y)	400 V
n	nominal rotor speed	1430 rpm
f	nominal frequency	50 Hz
$U_b = U_n$	reference voltage	400 V
$I_b = I_n\sqrt{3}$	reference current	19 A
P_b	reference power	7.6 kW

In Fig. 8, slow (1.5 s) revers of the IM from 0.1 to -0.1 p.u. is presented. The waveforms of estimated rotor speed $\hat{\omega}_r$, estimated rotor speed error $\tilde{\omega}_r$, s_ω from (29) and its filtrated value s_{ω_f}, estimated stator current error $\tilde{i}_{s\alpha}$, and T_e value for 1) $k_c = 0$, b) k_c is changed from 0 to 15. IM is loaded constant value of load torque $T_L = 0.7$ p.u.

For $k_c = 0$ the estimation error during IM revers is about 0.03 p.u. in the transient state and the steady state it is about 0.015 p.u. However, the value of estimated electromagnetic torque T_e is not properly estimated. This phenomenon is described in Section IV and has been shown in Fig. 2 (and it results from the shift error between estimated and real vectors). In this case [Fig. 8(a)], the error of the estimated stator current component has almost 0.1 p.u. Despite this, the observer is stable during the reversing with the nominal torque.

In Fig. 8 the waveforms of functions s_ω and its filtrated value $s_\omega \cdot f$ are shown. Close to zero rotor speed (from motoring to regenerating mode) in which the synchronous frequency is close to zero, the waveform of s_ω has oscillated (the same case is during the dynamic state). This function must be filtered and the filtered values should be introduced to (48) and to (28). Fig. 8(b) is the continuation of Fig. 8(a) but the value of k_c is changing from 0 to 15 p.u. to show how these values influence the improvement of observer properties.
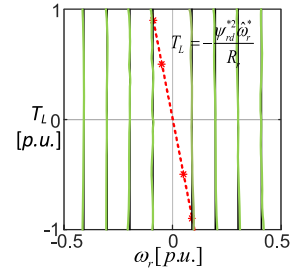
For k_c from 5.0 to 8.0 p.u. the electromagnetic torque T_e value is in the stationary state almost equal to T_L value. If the value of k_c is higher than 8.0 p.u. then the higher oscillations of T_e occur – what is visible in the other estimated variables [Fig. 8(b)], however, the estimated errors decay to zero.

In Fig. 9 the speed-torque trajectories for the NAFO structure are shown. Along the red line exist unstable poles of observer structure (the synchronous freq. is equal to zero).

In the next section, the theoretical analysis will be confirmed by experimental investigations.

VI. EXPERIMENTAL RESULTS

The experimental tests were carried out on a 5.5–kW drive system supplied by the voltage source converter (VSC). The electric drive system parameters are given in Table I. The control system was implemented in an interface with a *DSP Sharc* ADSP21363 floating-point signal processor and Altera Cyclone 2 FPGA. The transistor switching frequency was 3.3 kHz. The sampling time was 150 μs. The rotor speed was measured by the incremental encoder (11 bits) – only to the accuracy verification of observer structure. The stator current was measured by the current transducers LA 25-NP – in the phases "a" and "b" and transformed to the $(\alpha\beta)$ reference frame by using the Park transformation. The control system structure was presented in [16] and [20]. There are four classical PI controllers and the multiscalar transformation of variables [20] (description of the scheme is presented in the Appendix). The PI controllers and observer tuning gains are

TABLE II
TUNING GAINS OF SENSORLESS CONTROL SYSTEM

Name	k_{p11} [p.u.]	k_{i11} [p.u.]
x_{11} (ω_r)	6.0	0.01
x_{12}	5.0	0.028
x_{21} (ψ_r^2)	6.0	0.01
x_{22}	5.0	0.028
Speed observer tuning gains [p.u.]		
c_α	1.0	
c_ψ	0.2	
k_c	6.0 – 8.0	
γ (AFO)	0.8	
$1/T_i$ (s_ω filter)	0.005 – 0.01	

Fig. 11. IM is reversing from 1.0 to −1.0, nonloaded and the rotor speed value is estimated from (a) adaptive law (28), (b) nonadaptively (48).

Fig. 12. Measured load torque T_L during the rotor speed reverse (the waveforms from digital oscilloscope) for (a) AFO scheme, (b) NAFO scheme.
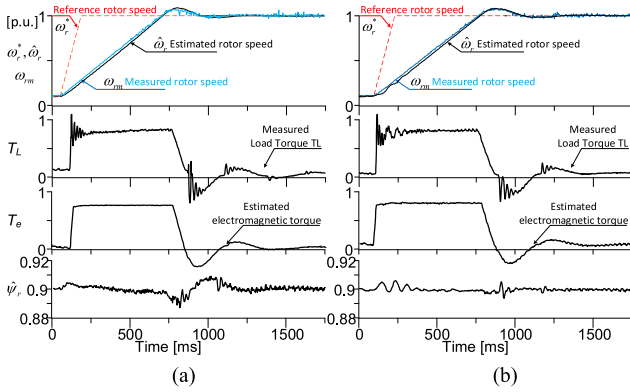

Fig. 10. IM is starting-up to 1.0, nonloaded and the rotor speed value is estimated from (a) adaptive-estimation law (28), (b) nonadaptively (48), the measured load torque T_L waveform is presented.

Fig. 13. (a) Rotor speed slow reverse from 0.1 to −0.1 p.u. for the NAFO estimation scheme (48). The machine is nominally loaded about $T_L = 0.75$ p.u.. (b) Regenerating mode of IM for the classical adaptive estimation scheme (28) and $k_c = 0$ during stationary state ($\omega_r = 0.08$ p.u.) and the load torque changes.

presented in Table II. In all tests, the reference square of rotor flux was $x_{21}{}^* = 0.9$ to 1.0 p.u. and the value of load torque was limited to $T_{Lmax} = 0.85$ p.u. The electromagnetic torque of IM is limited to 0.9 p.u. (the nominal torque is about 0.74 p.u.). Mainly, the following waveform of variables are shown: $\hat{\omega}_r$ – estimated rotor angular speed, $T_e = L_m L_r^{-1}(\hat{\psi}_{r\alpha}\hat{i}_{s\beta} - \hat{\psi}_{r\beta}\hat{i}_{s\alpha})$, $\hat{\psi}_r = \hat{\psi}_{r\alpha}^2 + \hat{\psi}_{r\beta}^2$ – electromagnetic torque and the square of rotor flux vector, $x_{22} = \hat{\psi}_{r\alpha}\hat{i}_{s\alpha} + \hat{\psi}_{r\beta}\hat{i}_{s\beta}$ – additional variable (in the stationary state $x_{22} \approx x_{21}/L_m$), i_m stator current vector module, $\tilde{\omega}_r = \hat{\omega}_r - \omega_r$ – estimated rotor speed error.

The experimental tests have been divided into three scenarios in which the results of AFO and NAFO are shown: 1st–Drive starting, speed reversal, very slow speed reverse (Section VI-A, Figs. 10 –13), 2nd–Load injections, and the regenerating mode of IM (Figs. 13 –15), 3rd–Uncertainties of IM parameters.

A. Drive Starting and Speed Reversal

The first scenario is presented in Figs. 10–13. In Fig. 10(a) the IM is starting-up to 1.0 p.u. for the adaptive speed estimation (AFO) law (28) and the same in Fig. 10(b), however, the speed is estimated nonadaptively from (48). In Fig. 11 the IM is reversing from 1.0 to −1.0 for both estimation schemes (28)—-Fig. 11(a) and (48)—-Fig. 11(b). In Figs. 10(a) and 11(a), the square or rotor flux vector components $\hat{\psi}_r$ has higher oscillations than in Figs. 10(b) and 11(b) for the nonadaptive rotor speed estimation
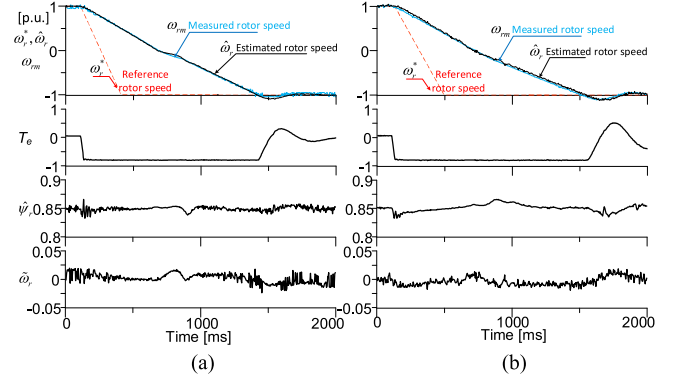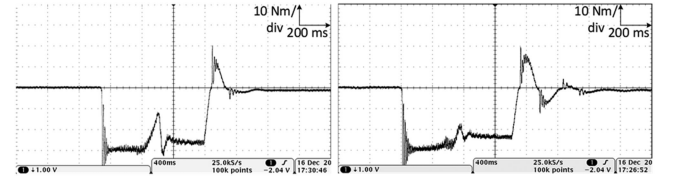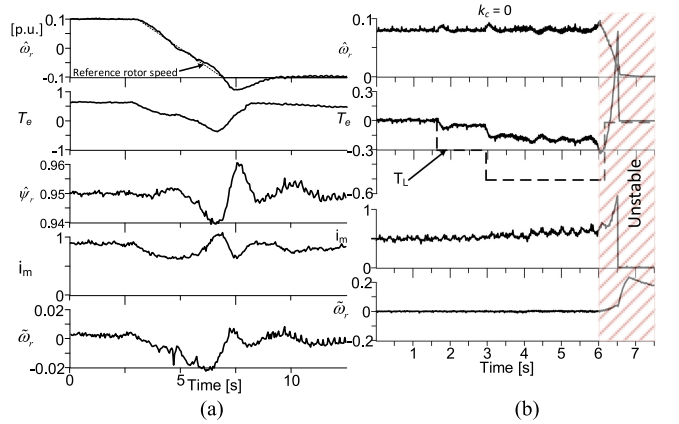
there are visible. The waveform of T_e is smoother in the adaptive law than nonadaptive. The response of T_e has smaller oscillations for adaptive than nonadaptive law. The estimated speed error has the same value smaller than 0.025 p.u. in transient states in both cases. In Fig. 12 the measured load torque T_L is presented during the rotor speed reverse from Fig. 11. There are visible load torque oscillations during the changes of the rotor direction (close to zero rotor speed). The load torque is measured by using a digital oscilloscope (analog signal from the torque meter). Fig. 13(a) presents that the rotor speed slow
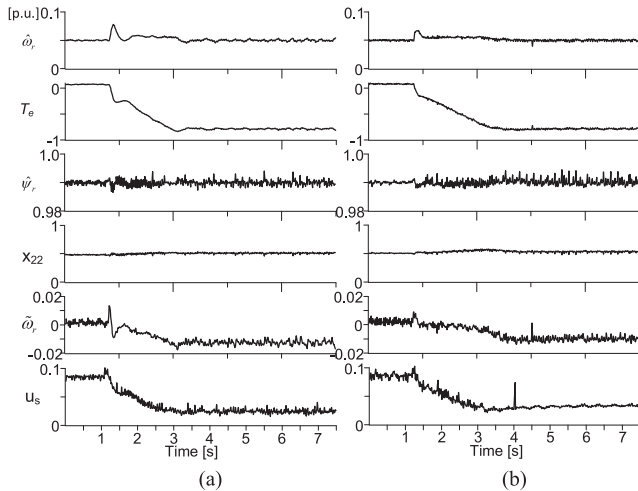
Fig. 14.   Regenerating mode of IM for (a) adaptive from (28), (b) non-adaptively (48). The rotor speed is set to 0.05 and load torque 0.75 p.u.
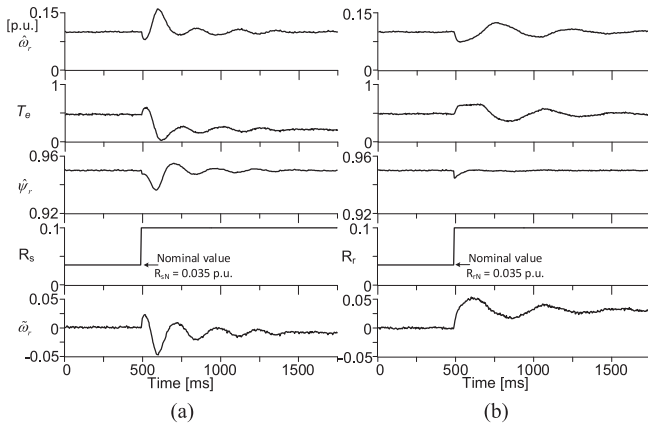

Fig. 15.   a) After 500 ms the nominal value of stator resistance is changed up to 0.1 p.u., the rotor speed is reproduced nonadaptively (48), the machine is loaded about 0.5 p.u.

reverses (about 4 s) from 0.1 to -0.1 p.u. during the IM loaded to about 0.75 p.u. is presented. The IM changes the operation mode from motoring (ω_r, T_e) > to regenerating ($\omega_r < 0$, $T_e > 0$).

The observer structure is stable, however, the estimated speed error increases up to -0.02 p.u. while the operating mode is changed.

In Fig. 13(b) the reference rotor speed is about 0.08 p.u. and the IM is step loaded (for regenerating operation mode). The classical AFO estimation scheme (28) is used. The proposed feedback is turned OFF ($k_c = 0$). If the load torque T_L is smaller than -0.25 p.u. the AFO is stable, but for a higher value of T_L the rotor speed has oscillations and the AFO is not stable [it is visible in Fig. 13(b)], and it confirms the theoretical stability analysis presented in Fig. 7(a) (for $k_c = 0$ the observer system has positive poles).

Experimental results Figs. 10–13(a) confirm that the sensorless control system with the proposed estimation schemes is stable during the dynamic states of IM.

Name	Classical AFO structure	AFO with feedback (28)	NAFO
Machine startup/reverse	stable	stable	stable
Avg. value of the maximum errors values of estimated rotor speed in the steady-state and low speed			
- regenerating mode	unstable	0.02 p.u.	0.018 p.u.
- machine mode	0.015 p.u.	0.015 p.u.	0.013 p.u.
Motoring operation mode	stable	stable	stable
Regenerating operation mode under nominal torque	unstable	stable	stable
(slow) IM reverse under nominal torque	unstable	sometimes unstable	sometimes unstable/better than AFO (28)
Zero speed and load torque	unstable	hold on the load torque	hold on the load torque
Very low-speed reverse	jerking around zero speed	smooth zero crossing	smooth zero crossing
Stable work during uncertainties	stable	stable	stable
Avg. val. of torque ripples in the steady state	0.047 p.u.	0.059 p.u.	0.067 p.u.

B. Load Injections and the Regenerating Mode of IM

In this scenario, the behavior of the speed observer system was checked during the constant rotor speed and changes of load torque values of IM (from motoring mode to regenerating mode). In Fig. 14 the rotor speed was set to 0.05 p.u. and after 1 s the IM is loaded about -0.75 p.u. (regenerating mode). The error of estimated rotor speed is about 0.01 in a stationary state. In addition to the previously presented variables the stator voltage, u_s are shown. The voltage u_s has a value of about 0.03 p.u., which gives about 12 V (the transistor's dead time is compensated). Nevertheless, the AFO with the proposed feedback function and the NAFO estimation scheme worked stable in regenerating operation modes.

C. Uncertainties of Parameters of IM

In this scenario, the behavior of the observer structure on changes of the stator and rotor resistance. The NAFO speed estimation scheme (48) was used during these tests. IM is loaded about $T_L = 0.5$ p.u.

In Fig. 15(a) the stator resistance is changed after 5 s ($R_s = 2.85 R_{sN}$). The rotor speed estimation error increases to about 0.015–0.02 p.u. The AFO structure errors are strongly dependent on the value of rotor resistance. In Fig. 15(b) the rotor resistance is changed from 0.035 to 0.1 p.u. ($R_r = 2.85 R_{rN}$). The

rotor speed estimation error increases to about 0.03 p.u. Despite the speed error, the T_e value is on the same level (about 0.5 p.u.).

Tests presented above confirm that the NAFO speed estimation scheme is robust on the uncertainties of nominal parameters of IM (of course at the chosen range). However, the estimation errors occurred, which was confirmed during the practical stability analysis (39). In Table III, the three structures of the speed observer are compared. The first one is the classical AFO with the adaptive law presented in [1]–[10] and (21), the second is AFO with the proposed robust feedback, and the third is the NAFO scheme.

VII. CONCLUSION

This article presents a nonadaptive speed estimation scheme for the classical AFO system (NAFO). Proposal 3 (Section III), shows that introducing the stabilizing function to the speed estimation formulae, which is based on the scalar product of the proper vectors, allows improving the performance and stability of AFO in the sensorless control structure. Furthermore, analysis of adaptive estimation with the integrator, presented in Section IV lead to the nonadaptive speed estimation scheme NAFO, which is the main contribution of this article. As a result, the estimation of rotor speed value without integrator was developed. The nonadaptive formula was based on the cross product as well as the scalar product of the two vectors in the system. Through this, the stability of the whole sensorless control structure was improved. The order of differential equations of the observer model was not increased as with other solutions presented, e.g., in the literature [9], [21]. Proposed solutions were tested in 5.5-kW IM supplied by VSC for the three scenarios (starting and reversing, load torque injections, and regenerating mode, nominal parameters uncertainties). Experimental results confirm that the proposed approach can be implemented in practical applications.

APPENDIX

In Table I the IM parameters are presented.

The sensorless control structure is presented in Fig. 16. This structure is based on multiscalar variables transformation [20], where $x_{11} = \hat{\omega}_r$, $x_{12} = \hat{\psi}_{r\alpha}\hat{i}_{s\beta} - \hat{\psi}_{r\beta}\hat{i}_{s\alpha}$, $x_{21} = \hat{\psi}_{r\alpha}^2 + \hat{\psi}_{r\beta}^2$, $x_{22} = \hat{\psi}_{r\alpha}\hat{i}_{s\alpha} + \hat{\psi}_{r\beta}\hat{i}_{s\beta}$. This control structure is studied in [16], [18], and [20].

In Table II the PI controllers from Fig. 16 and the observer structure tuning gains are presented.

In Table III the three estimation schemes of the rotor speed are compared. The first one is AFO with the classical adaptive law (21) (without robust feedback) [1]–[10], the second is the AFO with additional robust feedback law (28), and the third is the proposed nonadaptive scheme NAFO (48).

In Fig. 17 the experimental stand is shown. There are the IM coupled to the dc-machine, between both machines are two clutches and the torque meter.
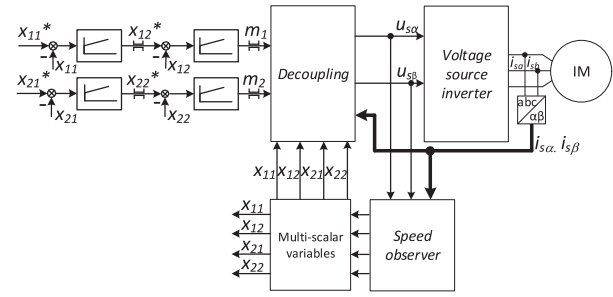

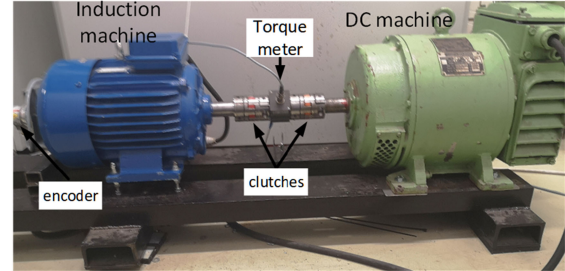Fig. 16. Sensorless control system scheme [20].

Fig. 17. Experimental stand with IM coupled to the dc-machine.

REFERENCES

[1] T. Orlowska-Kowalska, M. Korzonek, and G. Tarchała, "Stability analysis of selected speed estimators for induction motor drive in regenerating mode—A comparative study," *IEEE Trans. Ind. Electron.*, vol. 62, no. 10, pp. 7721–7730, Oct. 2017.

[2] M. Hinkkanen and J. Luomi, "Stabilization of regenerating-mode operation in sensorless induction motor drives by full-order flux observer design," *IEEE Trans. Ind. Electron.*, vol. 51, no. 6, pp. 1318–1328, Dec. 2004.

[3] H. Kubota, K. Matsuse, and T. Nakano, "DSP-based speed adaptive flux observer of induction motor," *IEEE Trans. Ind. Appl.*, vol. 29, no. 2, pp. 344–348, Mar./Apr. 1993.

[4] H. Kubota and K. Matsuse, "Speed sensorless field-oriented control ofInduction motor with rotor resistance adaptation," *IEEE Trans. Ind. Appl.*, vol. 30, no. 5, pp. 1219–1224, Sep./Oct 1994.

[5] S. Sunwankawin and S. Sangwongwanich, "Design strategy of an adaptivefull-order observer for speed-sensorless induction motor drive-trackingperformance and stabilization," *IEEE Trans. Ind. Electron.*, vol. 53, no. 1, pp. 96–119, Feb. 2006.

[6] H. A. Maksoud, S. M. Shaaban, M. S. Zaky, and H. Z. Azazi, "Performance andstability improvement of AFO for sensorless IM drives in low speedsregenerating mode," *IEEE Trans. Power Electron.*, vol. 34, no. 8, pp. 7812–7825, Aug. 2019.

[7] E. Etien, C. Chainge, and N. Bensiali, "On the stability of full adaptiveobserver for induction motor in regenerating mode," *IEEE Trans. Ind. Electron.*, vol. 57, no. 5, pp. 1599–1608, May 2010.

[8] C. Luo, B. Wang, Y. Yu, C. Chen, Z. Huo, and D. Xu, "Operating-point tracking method for sensorless induction motor stability enhancement in low-speed regenerating mode," *IEEE Trans. Ind. Electron.*, vol. 67, no. 5, pp. 3386–3397, May 2020.

[9] T. Orlowska-Kowalska, M. Korzonek, and G. Tarchała, "Stability improvement methods of the adaptive full-order observer for sensorless induction motor drive—Comparative study," *IEEE Trans. Ind. Informat.*, vol. 15, no. 11, pp. 6114–6126, Nov. 2019.

[10] W. Sun, K. Liu, D. Jiang, and R. Ou, "Zero synchronous speed stable operation strategy for speed sensorless induction motor drive with virtual voltage injection," in *Proc. IEEE Energy Convers. Congr. Expo.*, 2018, pp. 337–343.

[11] Z. Yin, G. Li, Y. Zhang, and J. Liu, "Symmetric-strong-tracking-extended-Kalman-filter-based sensorless control of IM drives for modeling error reduction," *IEEE Trans. Ind. Informat.*, vol. 15, no. 2, pp. 650–662, Feb. 2019.

[12] M. Bouheraoua, J. Wang, and K. Atallah, "Rotor position estimation of a pseudo direct-drive PM machine using extended Kalman filter," *IEEE Trans. Ind. Appl.*, vol. 53, no. 2, pp. 1088–1095, Mar./Apr.2017.

[13] M. Comanescu, "Design and implementation of a highly robust sensorless sliding mode observer for the flux magnitude of the induction motor," *IEEE Trans. Energy Convers.*, vol. 31, no. 2, pp. 649–657, Jun. 2016.

[14] M. Morawiec and A. Lewicki, "Application of sliding switching functions in backstepping based speed observer of induction machine," *IEEE Trans. Ind. Electron.*, vol. 67, no. 7, pp. 5843–5853, Jul. 2020.

[15] D. Traore, F. Plestan, A. Glumineau, and J. de Leon, "Sensorless induction motor: High-order sliding-mode controller and adaptive interconnected observer," *IEEE Trans. Ind. Electron.*, vol. 55, no. 11, pp. 3818–3827, Nov. 2008.

[16] M. Morawiec, "Z type observer backstepping for induction machines", *IEEE Trans. Ind. Electron.*, vol. 62, no. 4, pp. 2090–2103, Apr. 2015.

[17] C. Schauder, "Adaptive speed identification for vector control of induction motors without rotational transducers," *IEEE Trans. Ind. Appl.*, vol. 28, no. 5, pp. 1054–1061, Sep./Oct. 1992.

[18] Z. Krzeminski, "A new speed observer for control system of induction motor," in *Proc. IEEE Int. Conf. Power Electron. Drive Syst.*, 1999, pp. 555–560.

[19] P. Ioannou and J. Sun, *Robust Adaptive Control*. Englewood Cliffs, NJ, USA: Prentice Hall, 1996.

[20] Z. Krzeminski, "Nonlinear control of induction motor," in *Proc. 10th IFAC World Congr.*, Munich, 1987.

[21] J. Chen and J. Huang, "Globally stable speed-adaptive observer with auxiliary states for sensorless induction motor drives," *IEEE Trans. Power Electron.*, vol. 34, no. 1, pp. 33–39, Jan. 2019.

[22] J. Holtz, "Sensorless control of induction machines—With or withoutsignal injection?" *IEEE Trans. Ind. Electron.*, vol. 53, no. 1, pp. 7–30, Feb. 2006.

[23] H. Hofmann and S. R. Sanders, "Speed-sensorless vector torque control of induction machines using a two-time-scale approach," *IEEE Trans. Ind. Appl.*, vol. 34, no. 1, pp. 169–177, Jan./Feb. 1998.

Paweł Krolpewski received the M.Sc. degree in electrical engineering from the Gdańsk University of Technology, Gdańsk, Poland, in 2019.

His research interests include multiscalar models, nonlinear control of electrical machines, sensorless control, nonlinear control, and current source converters.

Ikechukwu Charles Odeh, received the Ph.D degree from the Department of Elect. Eng., University of Nigeria, Nsukka, Nigeria, in 2010.

From January to September 2011, he was a Visiting Scholar, sponsored by the United States Navy, with Tennessee Technological University, Cookeville, TN, USA. From July 2014 to October 2016, he was a Research Fellow, sponsored by the Alexandra Von Humboldt (AvH) Foundation, with the E.ON Energy Research Center, Rheinisch-Westfaelische Technische Hochschule (RWTH) Aachen, Germany. Since January 2020, he has been a Research Fellow, sponsored by the Polish National Agency for Academic exchange (NAWA) under the ULAM postdoctoral research grant, with the Faculty of Electrical and Control Engineering, Gdańsk University of Technology, Gdańsk, Poland.

Marcin Morawiec received the M.Sc. degree from the Czestochowa University of Technology, Czestochowa, Poland, in 2003, and the Ph.D. and D.Sc. degrees from the Gdańsk University of Technology, Gdańsk, Poland, in 2007 and 2017, respectively, all in electrical engineering.

Since 2017, he has been an Associate Professor with the Department of Electric Drives and Energy Conversion, Gdańsk University of Technology. He has authored over 70 articles, two monographs, two chapters in books, Polish patent, and five patent applications. His research interests include multiscalar models, nonlinear control of any electrical machines, sensorless control, nonlinear control, backstepping control, adaptive observer backstepping, and sliding mode.